

## Article

# The Latest Occurrence of *Stephanorhinus hundsheimensis* (Rhinocerotidae) in Europe: The Skeletons from the Cova del Rinoceront Site (Castelldefels, Barcelona)

David García-Fernández <sup>1</sup>, Esperanza Cerdeño <sup>2</sup> , Montserrat Sanz <sup>1,\*</sup>  and Joan Daura <sup>1,\*</sup> 

<sup>1</sup> Grup de Recerca del Quaternari (GRQ-SERP), Departament d'Història i Arqueologia, Facultat de Geografia i Història, Universitat de Barcelona, c/Montalegre, 6, 08001 Barcelona, Spain; davidapus@gmail.com

<sup>2</sup> Paleobiología y Paleoecología, Instituto Argentino de Nivología, Glaciología y Ciencias Ambientales (IANIGLA), CCT-CONICET-Mendoza, Avenida Ruiz Leal s/n, Mendoza M5500, Argentina; espe@mendoza-conicet.gob.ar

\* Correspondence: montsesanzborras@ub.edu (M.S.); jdaura\_lujan@ub.edu (J.D.)

**Abstract:** New rhino remains recovered from Cova del Rinoceront (Castelldefels, Barcelona) confirm the presence of *Stephanorhinus hundsheimensis* (Toula, 1902) at the site and the taxon's persistence until the late Middle–early Upper Pleistocene in Europe, that is, its latest documented occurrence. The three individuals recovered from the site are compared with specimens of other Pleistocene species, including those of *S. hemitoechus*, *S. kirchbergensis* and *Coelodonta antiquitatis*, but their anatomical characteristics (a long skull, moderate occipital elevation, partial nasal septum, and slender zygomatic arch) do not coincide with the latter's documented features. Certain similarities are found with the most frequently occurring rhinocerotid at that time in the Iberian Peninsula, *S. hemitoechus*, but the cranial features of the latter differ. The anatomical characteristics of the Cova del Rinoceront individuals coincide most closely with those of *S. hundsheimensis* (i.e., a high occipital face, with rounded proximolateral angles and oblique lateral borders, as well as the frontoparietal angle, and facial development). Despite the marked overlaps in the general measurements of *S. hundsheimensis* and *S. hemitoechus*, many (cranial and postcranial) dimensions of the Cova del Rinoceront individuals coincide more closely with those of the former, although some bone proportions are more similar to those of the latter specimens. Therefore, *S. kirchbergensis* and *C. antiquitatis* can be discarded as they tend to be larger, more robust species.

**Keywords:** rhinocerotids; mammals; Quaternary; MIS 5–6; Iberian Peninsula; Spain



**Citation:** García-Fernández, D.; Cerdeño, E.; Sanz, M.; Daura, J. The Latest Occurrence of *Stephanorhinus hundsheimensis* (Rhinocerotidae) in Europe: The Skeletons from the Cova del Rinoceront Site (Castelldefels, Barcelona). *Quaternary* **2023**, *6*, 60. <https://doi.org/10.3390/quat6040060>

Academic Editor: Miriam Belmaker

Received: 25 June 2023

Revised: 6 September 2023

Accepted: 22 November 2023

Published: 14 December 2023



**Copyright:** © 2023 by the authors. Licensee MDPI, Basel, Switzerland. This article is an open access article distributed under the terms and conditions of the Creative Commons Attribution (CC BY) license (<https://creativecommons.org/licenses/by/4.0/>).

## 1. Introduction

Europe's rhinocerotid record between the late Middle Pleistocene and the early Upper Pleistocene comprises three taxa: *Stephanorhinus hemitoechus*, *S. kirchbergensis*, and *Coelodonta antiquitatis* (e.g., [1,2]), with *S. hundsheimensis* being known to extend from the late Lower Pleistocene to the early Middle Pleistocene [2]. The most abundant of these species in the Iberian Middle–Upper Pleistocene localities is *S. hemitoechus* (e.g., [3–5]).

Recently, the number of Iberian localities correlated with marine isotope stage (MIS) 5 has increased thanks to improvements in radiometric dating methods. Examples include Gruta da Oliveira [6], Figueira Brava [7], Galería de las Estatuas (Atapuerca) [8], and Cueva del Camino [9]; other sites, in contrast, do not provide sufficient data for them to be correlated with any confidence to MIS 5 [10]. The palaeontological analyses conducted by Pandolfi and Tagliacozzo [11] (as detailed in [11] (Table 1)) also include the Spanish localities of Cueva del Castillo (Santander), Cueva del Congosto (Guadalajara), Villavieja (Castellón), and La Alfaguara (Granada). Within these sites, the rhinocerotid *S. hemitoechus* has been identified [3] during MIS 5. The presence of *S. kirchbergensis* during the late Middle Pleistocene–early Upper Pleistocene in Spain has largely been discarded [3,12], while that

of the woolly rhino (*Coelodonta antiquitatis*) has been recorded in the late Middle Pleistocene (MIS 6) in La Parte (Asturias) but is better known in Late Pleistocene localities ([13] and references therein).

In contrast, *S. hundsheimensis* has been recorded in Spain at Lower Pleistocene localities, including Vallparadís (Barcelona [5,14–17]), Incarcàl (Girona [18,19]—as *S. etruscus* [16,17]), and the Guadix-Baza Basin (Granada [20]—as *S. etruscus* [21–24]).

The rhinocerotid remains from Cova del Rinoceront were initially published as *S. etruscus brachycephalus* (mostly equivalent to *S. hundsheimensis*) by Daura and Sanz [25] and later ascribed to *S. hundsheimensis* [10]. The first remains were recovered from the rubble accumulated at the foot of the quarried face during the 2002 and 2003 field seasons. Here, a more complete sample, recovered in stratigraphic position, up to and including 2019, includes partial skeletons and allows us to revise the taxonomy, as well as the biostratigraphic and geographical implications, of this rhinocerotid material.

One complete and two partial skeletons have been recovered from layers III and VII of the sequence filling the Cova del Rinoceront site, which was possibly a natural pitfall trap [26]. Most of the rhino bones are anatomically connected, although two of the individuals were partially destroyed by quarrying activities. The completeness of the preserved remains provides new morphological data that enable us to extend previous comparisons and obtain a more accurate taxonomic determination, evaluated in the chronological context of MIS 5 and 6.

## 2. Cova del Rinoceront

### 2.1. Site Description

Cova del Rinoceront (henceforth, CR) is a cavity located in the municipality of Castelldefels (41°16′24.92″ N, 1°57′39.18″ E), some 25 km southwest of the city of Barcelona in northeastern Spain (Figure 1). The cave lies in the Garraf Massif, only 1 km inland from the extant seashore, at an altitude of 25 m abs. CR is in an abandoned quarry known as *ca n'Aymerich* and, as a consequence of quarrying activities, much of the site was destroyed in the 1960s and rubble accumulated at the base of the quarry face. This facilitated the identification of the site in 2002.

The cavity's infillings were exposed along a vertical section and were totally excavated between 2003 and 2023. The CR assemblage comprises, in the main, faunal remains, although a few stone tools have also been recovered. A multidisciplinary study of the cave [10] provided detailed data on its geology, archaeology, faunal composition, and chronology. The stratigraphic profile is 11 m thick and varies between 1.5 and 3 m in width. The sequence is composed of three main units (Units 1, 2, and 3), with eight differentiated layers (I to VIII) from the top to the bottom.

### 2.2. Stratigraphic Provenience and Chronological Framework of Rhinocerotid Remains

The rhinocerotid remains that constitute the focus of this contribution come from layer IIIe (basal part of layer III), the top of layer VII (Figure 1), and from the rubble accumulated at the foot of the quarry face. The reworked material from the latter originates mainly from layers I, III, and VI, but also from VII.

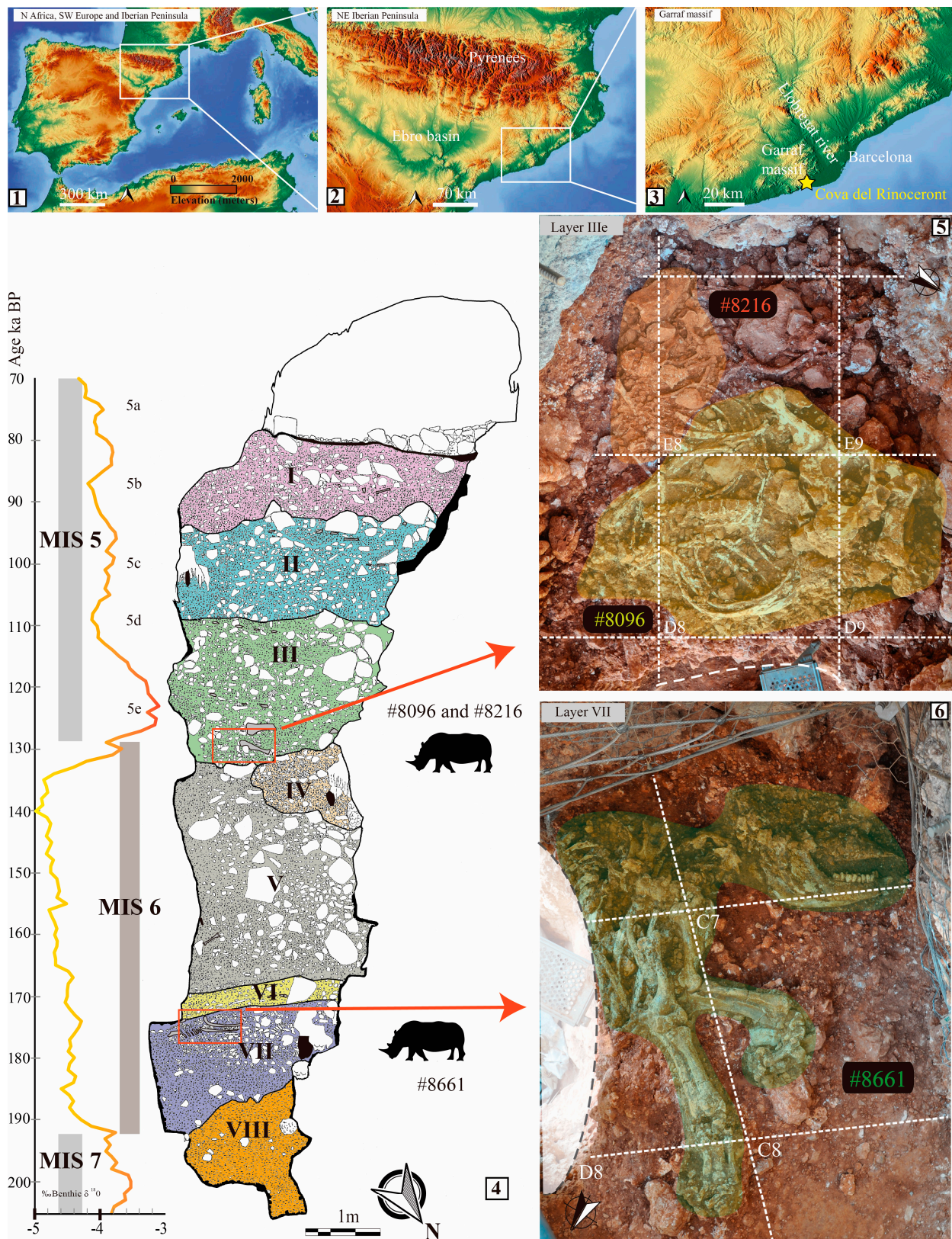


**Figure 1.** (1–3) Geographic location of the Cova del Rinoceront site in northeastern Spain (maps extracted from OpenStreetMap (CC BY-SA), OpenStreetMap© licensed under ODbL 1.0 by the OpenStreetMap Foundation (OSMF), ©OpenStreetMap contributors (<https://www.openstreetmap.org/>, accessed on 24 June 2023)); (4) stratigraphic sequence of differentiated layers; (5,6) details of the recovered rhinoceros individuals (# 8216, # 8096, and # 8661).

Layers III and VII are composed of clast-supported breccia. However, layer III is also constituted by large boulders (60–150 cm), gravels, and a sandy-silt matrix, while in layer VII boulders are present at the base, surrounded by a lutitic matrix with gravels, consisting of accumulations of subangular clasts coarsening upward. Both layers present a yellowish-red colouration according to the MUNSELL<sup>®</sup> soil colour chart (5 YR 5/8 for layer III and 5 YR 4/6 for VII). Several horizons (IIIa to IIIe) have been identified in layer III, four of which contain faunal remains: *Haploidoceros mediterraneus* [27] from the topmost sub-layer IIIa, a large number of specimens of *Testudo hermanni* from sub-layer IIIb, a complete skeleton of a *Palaeoloxodon antiquus* from sub-layer IIIc [28], and two rhinoceros individuals (# 8096 and # 8216) from the lowermost sub-layer IIIe [10].

The CR sequence is a well-dated deposit in the Iberian Peninsula with a total of 47 samples exposed to a range of geochronological methods (including, U-Th, luminescence, ESR, amino acids, and palaeomagnetism) that all place the site at between 74 and ~175 ka (layers I to VII) [10]. Rhinoceros individual # 8096 from layer IIIe has been dated two two times by means of the U-Th on bone (Mt III and ulna), giving ages (2- $\sigma$  confidence intervals) of 129.7 ka +3.7/−3.4 and 131 ka +16/−14 [10]. Thus, the chronology of the rhinoceroses (# 8096 and 8216) from layer III can be placed at the beginning of the Last Interglacial (MIS 5e), which is in agreement with the luminescence and uranium ages obtained for the layers underlying sub-layer IIIe. Rhinoceros individual # 8661, recovered from the basal layer of the sequence (layer VII), can be assigned to MIS 6, based on a speleothem dated from the cave wall covered by layer VII, with an age of 159.4 ka +12.1/−11, which provides a maximum age of ~171.5 ka (1- $\sigma$  confidence interval) or 183.6 ka (2- $\sigma$  confidence intervals) (see [10] for details). Luminescence ages obtained for the overlying layers are in agreement with this assignment.

### 3. Materials and Methods

The rhino remains from CR are stored at the La Guixera laboratory (Castelldefels City Council), having been excavated during fieldwork undertaken by the Grup de Recerca del Quaternari (GRQ-SERP, University of Barcelona). The assemblage includes both the remains from the rubble at the base of the cave, attributed primarily to sub-layer IIIe [10], and the remains in situ documented in anatomical position from sub-layers IIIe and VII. The two skeletons pertaining to specimens # 8096 and # 8216 from layer IIIe correspond to an adult and a juvenile (with milk dentition) individual, respectively. The juvenile (# 8216) constitutes a complete skeleton, but its preservation, enclosed in a hard breccia, prevents the separation of bones, which hinders their detailed description. In contrast, the adult skeleton (# 8096) has been partially destroyed by quarrying. However, fragments of skull, mandible, and isolated dentition, together with some postcranial bones, collected from the rubble, can be associated with individual # 8096 [10]. The third specimen, # 8661, recovered from layer VII, belongs to a sub-adult or young adult individual, and its postcranial skeleton is largely preserved in the matrix.

The taxonomic study of such remains is based on morphometric comparison and adheres to the methodology and terminology typically applied to this group of mammals (e.g., [1,29–31], among many others). The anatomical description considers six main planes for each element: proximal (dorsal in the skull), distal (ventral in the skull), anterior (to the head), posterior (occipital in the skull), medial (to the sagittal plane), and lateral (to the external side of the body). Limb bones are considered to be on the vertical axis, independent of their true anatomical position [29]. In the case of teeth, mesial and distal refer to the anterior and posterior faces, respectively. The comparative tables are included in Supplementary Online Material S1, while the bivariate plots are included in Supplementary Material S2 to show the proportions of the bones. Here, most comparisons are with other individual specimens (not with variation ranges) and are shown in accordance with the corresponding tables. Data for comparisons are drawn primarily from the literature as referenced throughout the text. Note that when citing Guérin's data [29] on *S. hundsheimensis*, we refer to material the author initially described as *Dicerorhinus etruscus brachycephalus*,

but later recognized as *S. hundsheimensis* [30]. Additional data on European localities, rhino species, and the associated bibliography can be consulted in a recently compiled database [32].

#### Anatomical Abbreviations

DP/dp: deciduous upper/lower tooth; M/m: upper/lower molar; Mc: metacarpal; Mt: metatarsal; P/p: upper/lower premolar.

#### 4. Systematic Palaeontology

Rhinocerotidae Gill, 1872

Rhinocerotinae Owen, 1845

Rhinocerotini Owen, 1845

*Stephanorhinus* Kretzoi, 1942

Type species: *Rhinoceros kirchbergensis* Jäger, 1839 [33]

*Stephanorhinus hundsheimensis* (Toula, 1902) [34]

##### 4.1. Referred Material

For individual # 8096, we refer to skull fragments, a left mandibular fragment with the p3–m2 (p4–m1 incomplete) and the p2 separated, a posterior fragment of a right lower molar, an isolated right P3 (incomplete), P4 and M3 (incomplete), a left M1 and M3, and numerous postcranial bones (long bones, metapodials, carpals, tarsals, and phalanges). For individual # 8216, the juvenile skeleton, we refer to material including the skull and mandible with milk dentition, and most postcranial bones. For individual # 8661, the sub-adult skeleton, we refer to materials including the skull and mandible with P/p2–M/m3 (P/p4 and M/m3 erupting; left Dp4 in place and right Dp4 separated), and most postcranial bones. The elements previously not assigned a collection number [10] (see [10] (Figure 7)) belong to # 8096, except for the tibia fragment (same side as the tibia of # 8096) which is here assigned to individual # 8661.

##### 4.2. Description and Comparison

###### 4.2.1. Skull

The skull fragments of # 8096, previously described in [10], present similarities and differences with both the skulls of *Stephanorhinus etruscus* and *S. hundsheimensis*; however, they were eventually assigned to the latter, based primarily on the occipital inclination and height. The skull of # 8661 is a more complete specimen, which, although belonging to a sub-adult (P/p4 and M/m3 not fully erupted, open sutures), allows a better comparative study to be undertaken.

The skull of # 8661, best preserved on its left side (Figure 2 (1)), is long, narrow, and relatively low. In lateral view, the dorsal profile presents a nasal convexity corresponding to the base of the nasal horn. Behind this, the profile appears to be concave, although this would seem to be overestimated by distortion, gently elevating to the occipital crest. The base of the frontal horn is less developed than that of the nasal horn. The specimen presents a short ossified nasal septum, fused to the premaxillaries, which are long and wider than the septum. The nasal cavity is elliptic, longer than it is high, while its end extends as far as the level of the distal half of the P4, well-separated from the anterior orbital border that is at the level of the M2–M3 (M3 starting to erupt). The oval infraorbital foramen is at the level of the P4–M1, below the nasal notch. The zygomatic arch is long, low, and slender. The supraorbital apophysis is short. The skull of # 8661 does not preserve the auditory region or the occipital area (in contrast with their good state of preservation in skull # 8096; Figure 2 (2)). In dorsal view, the insertion of the nasal horn is rugose, small, and elliptic, with the rugosity increasing laterally. The insertion of the frontal horn is barely swollen and less rugose. The preservation of the skull and mandible in anatomical position means the ventral side of the skull cannot be observed.

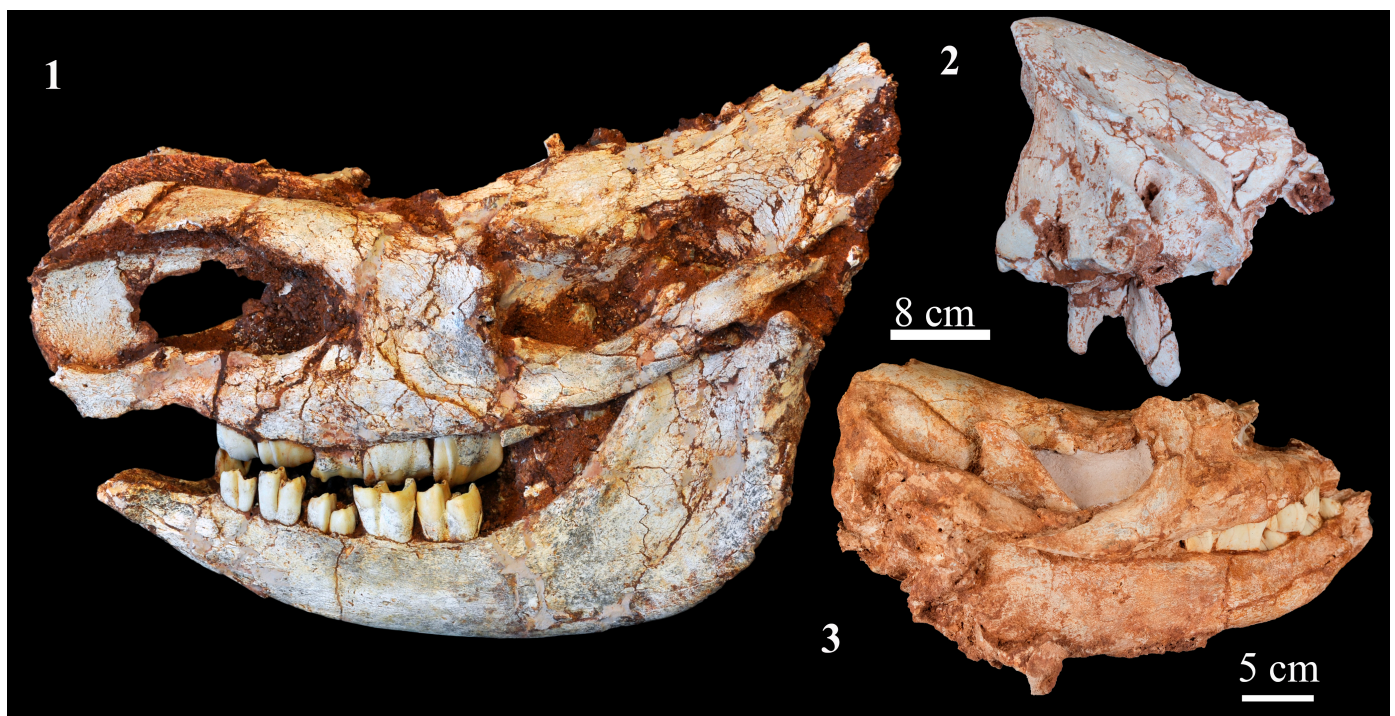


**Figure 2.** *Stephanorhinus hundsheimensis* from Cova del Rinoceront. (1) Individual # 8661, skull and mandible in anatomical position, left lateral view; (2) individual # 8096, posterior part of skull, right lateral view; (3) individual # 8216, skull and mandible in anatomical position, right lateral view.

In the posterior area of skull # 8096, the nuchal crest projects backward, without overpassing the level of the condyles (Figure 2 (2)); in dorsal view, the crest presents a median concavity [10] (see [10] (Figure 7 (6))). The fronto-parietal crests are well separated (46.2 mm); the parietals are smoothly convex. The external auditory meatus is ventrally closed, as the long, forwardly inclined postglenoid apophysis is in contact with the shorter post-tympanic apophysis. Both apophyses are wide and antero-posteriorly flattened, the latter forming a continuous complex with the paraoccipital apophysis. The occipital face is high and trapezoidal in outline, its dorsal profile hardly convex [10] (see also [10] (Figure 7 (6))). The lateral occipital crests are robust, with wide depressions for muscular insertion at the lateral side of each crest. The condyles are trapezoidal in outline. The left paraoccipital apophysis is shorter and narrower than the postglenoid apophysis, but well-projected from the condyle level.

The skull of # 8261 (Figure 2 (3)), being juvenile, is much smaller than the other two specimens. The nasal cavity is incomplete, the nasal notch reaches the level of the DP3, and the anterior border of the orbit reaches the level of the distal half of the DP4. No horn base has developed in the frontal, although this bone seems to be somewhat depressed due to dorsal pressure. This also occurs more posteriorly, resulting in dorsally prominent parietals.

The general aspect of skulls # 8661 and # 8096—long, with moderate occipital elevations, partial nasal septums, and slender zygomatic arches—means we can rule out their belonging to the Pleistocene taxa of *Stephanorhinus kirchbergensis* (which tends to have a larger, higher and more robust skull) and *Coelodonta antiquitatis* (which tends to present a complete nasal septum, larger horn bases, and an elevated, posteriorly extended dorsal profile) ([12,29,30,35]; among others)). Likewise, *S. hemitoechus* (e.g., [5,12,29,30,35–37]) differs in terms of presenting a larger, more developed nasal horn base, an elevated occipital area, with its nuchal crest stretched posteriorly, its parietal crests less separated and better differentiated (based on skulls in [36]), and a somewhat vertical occipital plane. In contrast, evident similarities can be found when comparing the two skulls (# 8661 and # 8096) with that of *S. hundsheimensis* (which likewise has many features in common with *S. etruscus*).

According to Fortelius et al. [30], however, *S. hundsheimensis* has more developed nasals and horn bases than those of *S. etruscus*. In this sense, the only moderate development observed in # 8661 could point to its belonging to this taxon; however, it should be borne in mind that this specimen corresponds to an individual that had not reached full adulthood. Interestingly, the nasal horn boss of # 8661 is comparable in terms of its development and position, with respect to the nasal tip and the septum, to that of the adult skull of *S. hundsheimensis* from Untermassfeld [38]. The frontoparietal angle 'n' (in lateral view; [31,39]) is around 150°, similar to the average value presented by *S. hemitoechus* according to Loose [39] (see also [5] (Figure 4G)). It is also similar to the angle presented by *S. etruscus*, but smaller than that of *S. hundsheimensis* (176° and 175°) according to Lacomat [31], although some specimens present smaller angles (e.g., [37] Figure 3E). Note, however, that the frontoparietal angle in # 8661 could be influenced by the dorsal distortion and might, therefore, have originally been larger. The general development of the facial region in # 8661 is more similar to this species, being larger than in *S. etruscus* [30,37]. The dorsal extension of the nasal septum and its general development are similar to those of *S. hundsheimensis* from Mosbach [29] (as *D. etruscus brachycephalus*) and Untermassfeld [38]. The position of the nasal notch is comparable to its usual position in *S. hundsheimensis* (posterior P4 to M1) [28–30], as observed, for instance, in the skulls from Mauer [40], Torrente Stirone [41] (as *S. hemitoechus*), and Frantoio [42], although this feature can vary. Similarly, the anterior border of the orbit is more similar to the position described in *S. hundsheimensis* (posterior level of the M2 [29,30,39]). The outline of the nasal cavity is very similar to that of the skulls from Mauer, Mosbach, Frantoio, Isernia [31], and Untermassfeld [38]. In occipital view, skull fragment # 8096 closely resembles the skull of *S. hundsheimensis* from Hundsheim [34], but the trapezoidal occipital face [10] (see [10] (Figure 7 (6))) seems to be somewhat higher. According to Lacomat [31], the rounded angles of the dorsal occipital border (slightly convex) and the oblique lateral borders (in contrast with the rather straight borders of *S. etruscus*) are a close match with those of *S. hundsheimensis*.

Size-wise, the skull dimensions fall within the range of values reported for *S. hundsheimensis* (Supplementary Material S1, Table S1). Specifically, the length from the nasal tip to the orbit in # 8661 is similar to the maximum values for both *S. hundsheimensis* and *S. hemitoechus*, while the distance from the nasal notch to the orbit is, in fact, greater than the maximum value for *S. hundsheimensis*, a species in which this measurement is proportionally shorter than in other *Stephanorhinus* [30] (see [30] (Figure 1)). However, the postorbital width in # 8096 is narrower than the minimum values for any of the species of *Stephanorhinus*, being closest to the smallest value reported for *S. etruscus*. Based on the measurements of # 8661, the relationship of the length nasal tip–orbit/length nasal tip–nasal notch presents a proportionally longer distance from the notch to the orbit than that found in other specimens of *S. hundsheimensis*, according to the bivariate plot in Kotowski et al. [38] (see [38] (Figure 7)), in which # 8661 would be most similar to some specimens of *S. kirchbergensis*. However, the subadult condition of # 8661 might have an influence on this proportional difference.

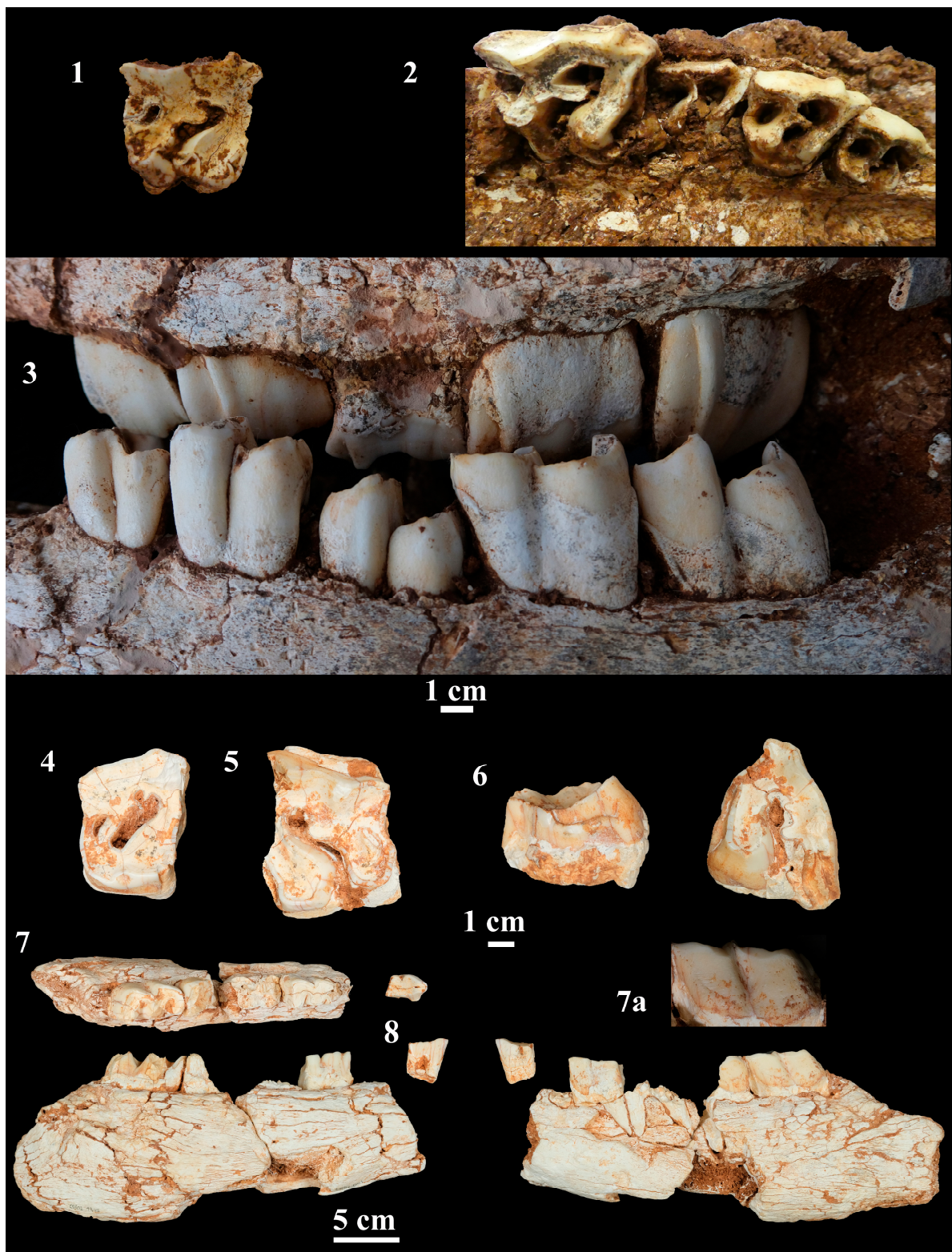


**Figure 3.** *Stephanorhinus hundsheimensis* from Cova del Rinoceront. (1) Right DP4 separated from skull # 8661, occlusal view; (2) right series P2-M1 of the skull # 8661, with permanent P4 ready to erupt, occlusal view; (3) left series P/p2-M/m2 (with upper DP4 still in place) of skull #8661, labial view; (4) right P4 of individual # 8096, occlusal view; (5) left M2 of individual # 8096, occlusal view; (6) left M3 of individual # 8096, mesial and occlusal views; (7) individual # 8096, left mandibular fragment with p3-m2 (p4-m1 broken), (7a) detail of labial face of m2 with horizontal grooves in the trigonid, and separated p2 (8) occlusal, lingual, and labial views.

#### 4.2.2. Mandible

The mandibles of individuals # 8216 and # 8661 (Figure 2 (1,3) and Figure 3 (3)), in anatomical position with their respective skulls, are slender, long, and low, tapering anteriorly. The ventral border is slightly, regularly convex, with a smooth inflexion below the m1–2 and without a marked angle in the symphyseal region (indeed, it presents barely more of an angle in the juvenile specimen). The posterior angle with the ascending ramus is also smooth, the entire ascending ramus being inclined backward. Part of the coronoid apophysis of # 8661 is curved backward, while the posterior border of the symphysis reaches the anterior level of the p2. The mental foramen is below the p2–3 level, and two other minor foramina are more anteriorly placed. The lateral face of the horizontal ramus is more convex in # 8661 than in the juvenile # 8261. The mandibular fragment of individual # 8096 [10] (see [10] (Figure 7 (1))) (Figure 3 (7)) is similar to the mandible of # 8661, but somewhat more robust, reflecting its older ontogenetic stage.

The position of the posterior border of the symphysis coincides with both those of *S. hundsheimensis* and *S. hemitoechus* [29], with only a small range of variation (p2–p3). The posterior inclination of the ascending ramus is also present in both species [29,30]. However, the mandible described by Cigala Fulgosi [41] as *S. hemitoechus* and reinterpreted as *S. hundsheimensis* [43] has a somewhat vertical ascending ramus. In general, the remains from CR are similar to those of *S. hundsheimensis* from Mosbach [44], Voigtstedt [45], Isernia [46], and Cesi [47]. Some mandibles of *S. hemitoechus* also present a ventral inflexion at a more anterior position, but others present the same condition, while the ascending ramus may or may not be more inclined [5,12]. The dimensions of the CR mandibles (Supplementary Material S1: Table S2) are mostly smaller than the mean values for *S. etruscus*, *S. hundsheimensis*, and *S. hemitoechus*, though some are higher than the mean of the former and some even below the minimum of the latter.

#### 4.2.3. Upper Dentition

A deciduous tooth (right DP4) is preserved in association with skull # 8661 (with the right P4 erupting), while the left DP4 remains in place (Figure 3 (1) and (2)). This indicates that individual # 8661 is younger than # 8096. The right DP4 (Figure 3 (1)) is rather square in outline, with a wide parastyle, an open V-shaped parastyle groove, and a narrow paracone fold projected forward, followed by an undulated wall. Cement remains are present inside the postfossette. The central valley is open almost to the crown base where the protoloph and metaloph converge. The crochet is large and rounded with a mesially directed inclination and a tiny crista. The protocone and metacone present anterior and posterior grooves, and a small antecrochet is well-delimited by the protocone's distal groove. A short mesiolingual cingulum is present at the level of the protocone's mesial groove. The most similar DP4s to those of our specimens are found in *S. hundsheimensis* from Süssenborn [48]. The DP4s from Untermassfeld present a smoother undulated ectoloph [49] while those from Vallonnet [50] and Voigtstedt [45] have a more labially oriented crochet.

In individual # 8661, the P2–3 are barely worn (Figure 3 (2)). Both are trapezoidal in outline, with narrow, well-projected parastyles. In P2, the parastyle presents an open U-shaped groove and the paracone fold is smooth. Occlusally, it presents an incomplete protoloph, which is not joined to the ectoloph at this wear stage. The P2 presents a prefossette, a small double crochet and a wide, deep, oval postfossette, and its lingual cingulum is continuous, fading at the posterolingual corner. In the P3, the paracone fold is more detached (a characteristic also observed in the erupting P4) and a subtle mesostyle is present. The labial enamel is vertically striated, while a long, thin crochet extends mesially almost reaching the protoloph, dividing the central valley into two large sections. The postfossette is relatively smaller than that in the P2. The lingual entrance of the central valley is wide and U-shaped at the junction of the protoloph and metaloph. This junction is above the lingual cingulum, which in common with the P2's cingulum is also continuous. The more easily observable right P4 presents a broken crochet. In the older, adult specimen # 8096, the P3 and P4 show a mesolabially-distolingually directed central fossette, the result

of the valley becoming closed. The crochet of the P3 is reduced to a crenulated border [10] (see [10] (Figure 7 (4))) whereas the P4 (Figure 3 (4)) presents a small, simple crochet placed rather labially and close to a short crista. The postfossette in the P4 is larger than in the P3 and labiolingually elongated, while in the P4 (P3 lingually incomplete), a weak cingulum develops at the base of the hypocone and the protocone-hypocone junction.

The molars (M1–2, but more easily observable in right M1) of individual # 8661 are trapezoidal in outline, with cement remains (Figure 3 (2) and (3)). As the M2 is barely worn, its occlusal face is shorter and narrower than that of the M1, but both diameters increase with wear. The parastyle is acute and moderately projected, the paracone fold is narrow and there is a marked wide mesostyle, so that the ectoloph is rather undulate. The crochet is long and extends mesially, while the postfossette is trapezoidal in outline. The central valley is very deep, with a narrow, V-shaped lingual entrance. The mesial cingulum is thick and extends lingually reaching the entrance of the central valley. The enamel is slightly rugose. The M2 of # 8096 (Figure 3 (5)) is a worn tooth, but the median valley is still lingually open. It bears a large, rounded crochet, while the area of the crista is incomplete. The M3 of # 8096 (Figure 3 (6)) presents a convex ectometaloph, with a wide, little projected paracone fold. The protocone is differentiated by its shallow anterior and posterior grooves. The molar presents one short, rounded crochet, and a second one, more labially placed and less developed that could be homologous to the crista of the M1–2. There is also a poorly developed antecrochet, close to the labial corner of the valley. The mesial cingulum is low and thick.

The ectoloph profile of individual # 8661 coincides largely with that of the P2–M2 of *S. hundsheimensis* from Vergranne [29]. Here, the premolars of specimens # 8096 and # 8661 both present occlusal features similar to those from Voigtstedt, Süßenborn [48], and Isernia [46], among others; yet, more developed cristae (double in the case of Voigtstedt) and multiple crochets may be present. Molar features, likewise, mostly coincide with those of *S. hundsheimensis* [34,38,41,45,46,48,51]. The presence of antecrochet in the M3 is occasional in *S. hundsheimensis* and *S. etruscus* (e.g., [52]). The ectoloph profile in *S. hemitoechus*, primarily in the P4, differs in terms of presenting a more undulate relief [29], a narrower and more projected parastyle, with a deeper parastyle groove, and a differentiated metacone fold [3,53].

Size-wise, most upper dental dimensions lie within the range reported for *S. hundsheimensis* (Supplementary Material S1: Table S3); however, the coincidences with the dimensions reported for *S. hemitoechus* are fewer.

#### 4.2.4. Lower Dentition

In individual # 8661 (Figure 3 (3)), the triangular p2 presents finely striated labial enamel whereas it is smooth in # 8096 (Figure 3 (8)). The paralophid extends mesially and in the unworn p2 of # 8661 it limits an open valley that almost disappears with wear, a feature also observed in # 8096. In occlusal view, the labial groove is V-shaped, becoming shallower to the base of the crown. The labial convexity of the trigonid and talonid is more evident in # 8661, while the trigonid is more flattened mesially in # 8096. The occlusal surface of the p2 in # 8096 forms an inclined plane, presenting a somewhat convex-concave curve (as seen in the labial view). In the lingual view, the mesial half of the tooth is higher than the distal half. The unworn p3 is similar to the p2, but the trigonid encloses a more developed valley. Anterior and posterior V-shaped valleys are equally deep in # 8661. The erupting p4 in # 8661 presents a prominent angled protoconid, whereas in the worn p4 of # 8096, the anterior valley is quite small and the labial walls are more flattened. The m3 of the latter individual presents a wider, deeper labial groove than that of the p4, while the V-shaped valleys present a slight difference in depth. In this tooth, several horizontal grooves on the labial face of the trigonid (Figure 3 (7a)) may be indicative of hypoplasia. The erupting m3 in # 8661 only allows us to observe the paraconid and protoconid cusps. All teeth present cement remains.

The morphology described coincides primarily with that of *S. hundsheimensis* [30,51,54], albeit the latter presents some variation in terms of the level of the valleys [45,51]. In *S. hemitoechus*, the hypolophid joins the trigonid more lingually.

The size of the lower dentition of individual # 8661 falls within the ranges reported for both *S. hundsheimensis* and *S. hemitoechus*, but most measurements coincide better with those of the former, with some values below its minimum values, while they are more dissimilar to those of *S. hemitoechus* (Supplementary Material S1: Table S4). The isolated lower teeth of *S. hundsheimensis* from other Spanish localities [20] present some variation, with the p2 and p3 from Fuente Nueva-3 proportionally narrower than those in # 8096, but all teeth are of a similar general size. Similar or slightly higher values are observed in the case of the Spanish *S. hemitoechus* [3,55–57].

#### 4.2.5. Fore- and Hindlimb Long Bones

Long bones have been recovered for all three individuals; however, as discussed, many skeletal elements of individuals # 8661 and # 8216 are embedded in the sedimentary matrix and cannot be described adequately (Figure 1 (5) and (6)).

In accordance with the sub-adult age revealed by its dentition, the suture of the humeral head of # 8661 (Figure 1 (6)) is not fully fused. The right humerus of # 8096 is complete (Figure 4 (1)), though fractured. Both bones present a well-developed deltoid tuberosity, their distal end extending to reach half of the diaphysis. This tuberosity, however, seems to be more vertical than that in the humerus from Hundsheim [34]. The greater tubercle is more extended laterally than proximally. The distal epiphysis is moderately widened (Supplementary Material S1: Table S5), the trochlea is asymmetrical, while the medial lip is higher and more extended transversely. The general dimensions match well with those of *S. hundsheimensis*, though the diaphysis is proportionally wider than that in the specimens from Soleilhac (Supplementary Material S1: Table S5; Supplementary Material S2).

The femur of individual # 8096 (Figure 4 (2)) presents a marked medial concavity in the shaft and a low, laterally extended third trochanter. The head and the greater trochanter are practically at the same level, the former barely separated from it, with no neck having developed. The distal trochlea is asymmetrical (medial lip poorly preserved) and wide. A juvenile distal fragment recovered from the rubble likely belongs to individual # 8661. The femur of # 8096 is proportionally shorter than that of the specimens in the comparative study (Supplementary Material S1: Table S6); for instance, the femur from Untermassfeld, while presenting a similar transversal diameter of its diaphysis (69 mm), is clearly longer (496 mm vs. 431 mm). Thus, the femur of # 8096 is more robust.

The radius and ulna of # 8661 (Supplementary Material S1: Table S7) are in anatomical connection with the humerus. The distal epiphysis of the radius is not completely fused. The radius of # 8096 (Figure 4 (3)) has a rather straight diaphysis, with both epiphyses extending a little laterally, affording it a concave lateral profile in anterior view, but less markedly than in the radius from Hundsheim [34] or in that reported by Cigala Fulgosi [41]. The olecranon of the ulna is robust (Figure 4 (3)), and not especially curved medially.

The fractured right tibia of individual # 8096 (Figure 4 (4); Supplementary Material S1: Table S8) is more robust than the radius. The transversal diameters (epiphyses and diaphysis) are relatively large compared to those of other specimens of *Stephanorhinus* (Supplementary Material S2). The lateral proximal facet for the tibia projects proximally, which is more evident in the posterior view. The intercondylar area is relatively wide. The tibial tuberosity is proximally blunt and the crest forms a smooth lateral concavity in the anterior view. The groove of the tuberosity (*sulcus extensorius*) is wide and high. The fibula is preserved in anatomical position with the tibia but is incomplete.



**Figure 4.** *Stephanorhinus hundsheimensis* from Cova del Rinoceront, individual # 8096. (1) Right humerus, proximal, anterior, posterior, and distal views; (2) right femur, proximal, anterior, posterior, and distal views; (3) right ulna and radius in anatomical position, though somewhat displaced, anterior, posterior, and medial views; (4) right tibia and fibula in anatomical position, anterior, distal, proximal, and posterior views.

Incrusted into the medial proximal facet of the tibia is a displaced sesamoid bone (Figure 4 (4)), suggesting the possible presence of a knee-joint sesamoid embedded in the gastrocnemius or popliteus muscles (known as fabellae—lateral and medial—and cyanella, respectively, sometimes appearing fused), considering that skeleton # 8096 was found predominantly in anatomical connection. Sesamoids of this type are common in different groups of mammals (e.g., Carnivora, Primates), but have rarely been described in fossils. However, studies, both old and more recent, signal that sesamoids of the knee-joint are not present in ungulates, which prevents an accurate interpretation here (see [58] for a summary of the development of sesamoids in tetrapods). Its possible presence in this rhinoceros would be a novelty requiring further study before being confirmed.

#### 4.2.6. Carpal Bones

The following description corresponds to individual # 8096: The scaphoid (Figure 5 (1)) is a high bone, slightly higher posteriorly. The trapezoidal medial face is slightly convex antero-posteriorly, with a crest delimiting a wide, shallow groove at the basal third of the bone. The proximal facet is triangular in outline and mainly concave, with an anteriorly convex area. The anteromedial border forms a medially concave–convex curved profile, with a strong slope, forming a short apophysis. Distally, three facets are continuous, but differentiated by strong crests: the smallest and most posterior corresponds to the trapezium and is slightly concave, the other two, corresponding to the trapezoid and magnum, are much larger and saddle-shaped, the latter proportionally longer and subtriangular. Laterally, the semilunate presents two large facets, and the proximal facet is subdivided by a subtle vertical crest and forms a right angle with the proximal articulation. Separated by a wide, deep rectangular groove, the semilunate's distal facet is subrectangular and smoothly curved, and almost forms a right angle with the magnum facet. Among the *S. hundsheimensis* specimens, the most similar bones are those recovered from Voigtstedt, Süssenborn, Untermassfeld, and the Yerevan Cave [45,48,49,59]. The carpal bones of *S. hemitoechus* from the Spanish site of La Cova del Gegant [3,60] present a more convex posterior border and the proximal articulation is trapezoidal and more massive, as in other specimens of this species [31]. Size-wise, the dimensions of individual # 8096 are, in the main, similar to the mean values of *S. hundsheimensis*, though the size of this species overlaps considerably with that of *S. hemitoechus* (Supplementary Material S1: Table S9).

The semilunate (Figure 5 (2)) presents a subtriangular anterior outline, proximally wide and pointing distally, with a lateral constriction. The convex proximal articulation does not extend posteriorly over the posterior apophysis. Medially, the scaphoid's proximal facet is triangular and flattened, while the distal facet is narrower and subdivided into two surfaces at an obtuse angle: an anterior triangular area and a low, long posterior extension. Above the border of the latter, a hole with a thin median septum could be indicative of biological activity (Figure 5 (2)). The pyramidal bone has two lateral facets: the proximal facet is relatively short and subtriangular, forming an obtuse angle with the proximal articulation of the radius; the distal facet is long, with a median inflexion on its proximal border, creating the appearance of two united crescents (Figure 5 (3)). The anterior part of this facet forms a marked angle with the distal articulation of the unciform. In the distal view, the two facets (of the magnum and unciform) form an obtuse angle ( $210^\circ$ ), leaving a curved crest in between. The magnum facet (medially located) is subrectangular, longer, and antero-posteriorly convex; the unciform facet is oval, pointing posteriorly, shorter, and more concave (Figure 5 (6)). The dimensions of the semilunate (Supplementary Material S1: Table S10) fall within the range reported for *S. hundsheimensis* [29,31,49], while the semilunates of *S. hemitoechus* present proportionally wider bones (e.g., Valle Radice [11], La Cova del Gegant [3,60]).

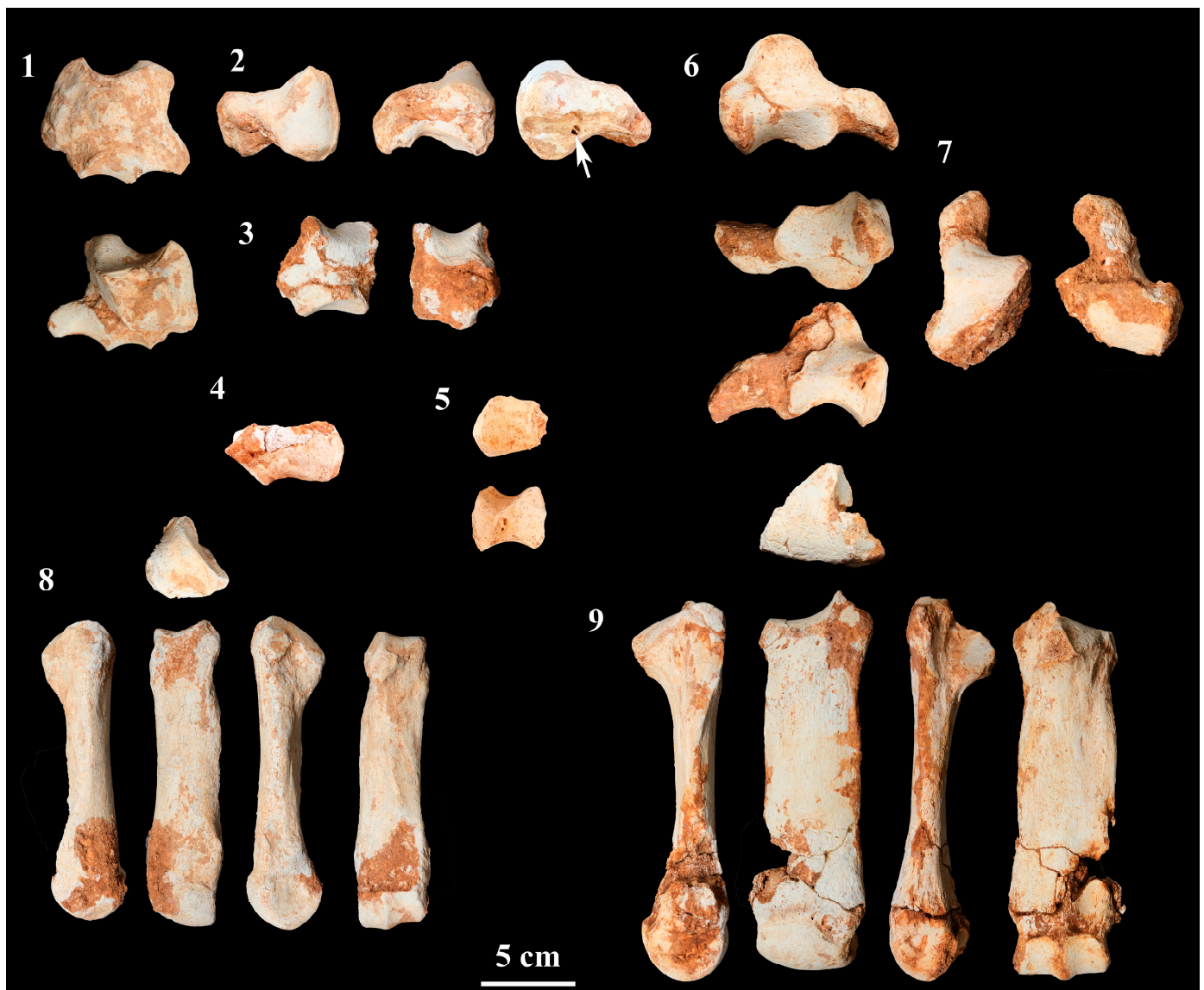


**Figure 5.** *Stephanorhinus hundsheimensis* from Cova del Rinoceront, individual # 8096. (1) Left scaphoid, anteromedial and posterolateral views; (2) right semilunate, proximal, lateral, and medial views (bioerosion marked by arrow); (3) left pyramidal, posteromedial and anterolateral views; (4) pisiform; (5) trapezoid; (6) right magnum, lateral, distal, and medial views; (7) right unciform, proximal and distal views; (8) left Mc II, lateral, anterior, medial, and posterior views, and proximal view above the anterior one; (9) left Mc III, medial, anterior, lateral, and posterior views, and proximal view above the anterior one.

The pyramidal is a relatively high bone. The proximal facet of the ulna is large, saddle-shaped, and a little narrower posteriorly than anteriorly. The medial face is slightly convex as are the facets for the semilunate: the crescent-shaped, proximal facet is smoothly continuous with the ulnar articulation, while the L-shaped distal facet forms an acute border with the distal articulation for the unciform. Both facets are well-separated by a wide, subrectangular depression. The pisiform facet is located on the posterior tuberosity of the bone. The distal facet for the unciform is antero-posteriorly concave and transversely flattened. Similarities are evident with the specimens of *S. hundsheimensis* from Soleilhac and Untermassfeld [30,31,49]. *S. hemitoechus* differs in having a more developed posterior tuberosity. Pyramidal dimensions are similar to those of *S. hundsheimensis*, while *S. hemitoechus* presents higher mean values (Supplementary Material S1: Table S11).

The pisiform is long, low, and narrow (Figure 5 (4)), bearing two anterior facets (the ulna and the pyramidal) located at a great angle. The ulnar facet is larger and flattened whereas the pyramidal facet is slightly convex. Behind the articular area, the long posterior apophysis is rather rectangular in outline and does not widen proximodistally. In general, *S. hundsheimensis* has larger apophyses [29,30], but the pisiform studied here is similar to that from Untermassfeld [49]. Size-wise, the general dimensions are similar to those of the pisiforms from Soleilhac and Isernia (Supplementary Material S1: Table S12).

In the case of the trapezoid (Figure 5 (5)), the proximal facet of the scaphoid is antero-posteriorly concave and transversely convex. The distal articulation is oval and less concave. The medial facet of the trapezium occupies the entire height of the posterior half of the face, with its anterior border limiting a rugose surface. Laterally, most of the face is occupied by the facet for the magnum. The specimen greatly resembles those of *S. hundsheimensis* from Vergranne [29] and Yerevan [59]. In *S. hemitoechus*, the distal articulation is subtriangular and extended laterally (e.g., La Cova del Gegant [60]). The length and height of the trapezoid are both below the minimum values of *S. hundsheimensis* based on the observations of Guérin [29], while the length and width of the trapezoid are smaller than those of the specimens from Vallonnet and Pietrafitta (Supplementary Material S1: Table S13). In the case of *S. hemitoechus*, the most similar specimens are those from Cova del Gegant [60] and Orgnac [31].

The magnum (Figure 5 (6)) is antero-posteriorly long, with a strong posterior apophysis. The anterior face is low, pentagonal in outline, with a convex base. The proximal protuberance is high and very convex and bears the facet for the pyramidal. Medially, there is a small, sub-squared facet for the trapezoid, which is anteriorly placed. The medial depression is wide. Laterally, two large facets articulate with the unciform (the most proximal of the two) and the Mc IV (the most distal). They are continuous, with a smooth crest in between, and the Mc IV facet being more extended posteriorly. In this face, there is an irregular depression behind the facets. The distal articulation for Mc III is trapezoidal in outline, antero-posteriorly long, pointed posteriorly, with a medial concavity. The posterior apophysis is posterodistally curved, more convex medially than laterally, and well-differentiated from the main corpus of the bone. The magnum is very similar to those of *S. hundsheimensis* from Voigtstedt, Isernia, and Untermassfeld [45,46,49]. *S. hemitoechus* presents a more rhomboidal anterior face [29–31]. The size of the magnum is similar to that of *S. hundsheimensis* (Supplementary Material S1: Table S14), larger than the specimen from Soleilhac and more similar to the smallest ones from Untermassfeld. It also presents similar values to those of the mean of *S. hemitoechus* based on data in Guérin [29], and greater values than those presented by the Spanish specimens from Lezetxiki and La Cova del Gegant [3,60].

The unciform (Figure 5 (7)) presents a rather square anterior face, higher and more convex laterally than medially and with a basal median inflexion. The convex proximal facet for the pyramidal extends anteriorly and is slightly concave transversally. The medial facet of the magnum forms a right angle with the proximal facet. The distal articulation gathers two large facets for the Mc III and Mc IV, differentiated by an incomplete crest. The area for the Mc IV is narrower and placed postero-laterally to the Mc III facet. The morphology is very similar to that of *S. hundsheimensis* from Soleilhac [29] (see [29] (Figure 92)). The size coincides with that of a specimen from Isernia, but the dimensions of the *S. hundsheimensis* and *S. hemitoechus* overlap widely (Supplementary Material S1: Table S15).

#### 4.2.7. Metacarpals

The Mc II is narrow proximally but progressively widens distally (Figure 5 (8)). The proximal facet of the trapezoid is subtriangular, with a convex mesial border. It is smoothly concave transversely and convex antero-posteriorly. In the anterior view, the medial articulation of the magnum is a flattened, sub-rectangular strip at an obtuse angle with the proximal facet. At each end, the magnum extends in two facets of the Mc III, well-separated from each other, the anterior facet being longer and more rounded than the posterior facet (Figure 5 (8)). In the posterior view, two crests diverge distally from the proximal edge, one of these crests extends medially whereas the other extends along the posterior face

to the distal epiphysis (Figure 5 (8)). In the distal epiphysis, the epicondylar width is hardly greater than that of the trochlea. The morphology described coincides with that of *S. hundsheimensis* from Voigtstedt [45], Untermassfeld [49], and Soleilhac [29] (see [29] (Figure 95A1)). *S. hemitoechus* presents a smaller distal epiphysis and a shorter antero-posteriorly proximal epiphysis that are more regular and have a more convex medial border [29] (see [29] (Figure 95C2)), [11] (see [29] (Figure 4a,d,g)). The length of the Mc II is shorter than the minimum value of *S. hundsheimensis* according to data from Guérin [29] and Fortelius et al. [30], while it is close to the maximum of *S. hemitoechus* according to Guérin [29], being quite similar in this regard to the Spanish specimens from Cueva del Camino-Pinilla del Valle (Supplementary Material S1: Table S16). Its gracility index is similar to that of some specimens of *S. hundsheimensis*, including that from the type locality, Hundsheim, and also to the least robust Mc II of *S. hemitoechus* (Supplementary Material S1: Table S16, Supplementary Material S2).

The Mc III (Figure 5 (9)) also widens progressively to the distal epicondyles. In the anterior view, the proximal facets form an elevated, acute crest. The magnum facet is large, triangular in outline, with a lateral notch, and is antero-posteriorly convex. The unciform facet is smaller, subtriangular, and smoothly concave antero-posteriorly. The lateral facets for the Mc IV are well-separated from each other: the anterior facet forms an angle of around  $110^\circ$  with the unciform-facet, while the posterior facet is oval and proximodistally higher. The diaphysis has an almost elliptic median section. The distal width at the epicondylar level is greater than that of the trochlea. The dimensions of the Mc III lie within the range of values presented by *S. hundsheimensis* and *S. hemitoechus*, but are, in general, below the mean values of the latter, with the exception of the length. However, the length of the Mc III is smaller than that of the three Spanish specimens, which means it is a more robust bone. Indeed, its gracility index is slightly higher than those in other specimens of *S. hundsheimensis*, but more similar to the values of *S. hemitoechus* (Supplementary Material S1: Table S17, Supplementary Material S2).

The Mc IV of # 8096 preserves its proximal area, the diameters of which are slightly smaller than those of the Mc IV from Hunsheim and very similar to the maximum values presented by those from Mosbach (Supplementary Material S1: Table S18). Individual # 8661 preserves all its metacarpals in anatomical connection (Figure 1 (6)) and cannot, therefore, be adequately measured. However, its Mc IV is curved with the diaphysis laterally concave.

#### 4.2.8. Tarsal Bones

The astragalus and calcaneus of individual # 8096 are anatomically connected (Figure 1 (5)). The astragalus is longer than it is high, while the trochlea is asymmetric, with the lateral area presenting a smooth slope in contrast to its steeper medial area. A short but nitid neck separates the trochlea from the distal articulation. The latter is composed of a large navicular facet and a narrow cuboid facet, forming a marked angle. The calcaneus facets are not observable. In the posterior and lateral views, the calcaneus is robust with a wide tuber and little narrowing below it. The sustentaculum is long and forms an obtuse angle with the corpus of the bone. The distal facet of the cuboid is subtriangular, transversely concave, and has a convex lateral border. Both tarsal bones are similar to the homologous specimens from Hunsheim [34], though there are some discrepancies in their relative measurements (e.g., a marked difference in the anteroposterior diameter of the tuber calcis). In contrast, the measurements coincide with those of other specimens of *S. hundsheimensis* (Supplementary Material S1: Tables S19–S20).

The cuboid is a short, wide bone, not antero-posteriorly deep, and quite robust (Figure 6 (2)). The posterior apophysis is wide but does not expand much either posteriorly or distally. Proximally, the calcaneus facet is wider and antero-posteriorly shorter than the astragalus facet. The navicular (Figure 6 (3)) is subrectangular, deeper than it is wide, and regularly concave proximally. Distally, the entocuneiform facet inclines postero-proximally. The mesocuneiform facet is suboval and slightly larger, while the L-shaped

ectocuneiform facet is the largest distal facet. The anterior face of the ectocuneiform (Figure 6 (4)) is quite straight except for its lateral end, where it curves posteriorly. Its lateral notch is well marked and its posterolateral corner defines an obtuse angle with the latero-posterior facet of the cuboid. The measurements of these tarsals are listed in Supplementary Material S1 (Tables S21–S25). The cuboid is relatively small with respect to the samples in the comparison. For instance, the anteroposterior diameter coincides with the minimum value obtained by Guérin [29] for *S. hundsheimensis*. The size of the navicular falls well within the range for this species, being most similar to those from Soleilhac. The entocuneiform is quite large and proportionally higher (Figure 6 (5)); indeed, its height is similar to the maximum value obtained by Guérin [29] for *S. hundsheimensis*, and is greater than that of the largest specimen from Isernia (which is longer and wider) and those from Untermassfeld (slightly wider). The size of the mesocuneiform corresponds to the average values obtained by Guérin [29], and the entocuneiform is proportionally longer than the specimen from Pietrafitta.



**Figure 6.** *Stephanorhinus hundsheimensis* from Cova del Rinoceront, individual # 8096. (1) Right calcaneus and astragalus in anatomical position, lateral, anterior, and distal views; (2) right cuboid, proximal, medial, and distal views; (3) right navicular, proximal, lateral, and distal views; (4) right ectocuneiform, proximal, lateral, and distal views; (5) right entocuneiform, posterior view; (6) right Mt II, lateral, anterior, medial, and posterior views, and proximal view above the anterior one; (7) right Mt III, medial, anterior, lateral, and posterior views, and proximal view above the anterior one; (8) right Mt IV, lateral, anterior, medial, and posterior views, and proximal view above the anterior one.

#### 4.2.9. Metatarsals

The right and left metatarsal bones of # 8096 are relatively slender. Mt II (Figure 6 (6)) presents a deep (anteroposterior), narrow proximal epiphysis that is medially convex; the proximal facet is subtriangular and transversely concave. On its lateral face, the anterior facet for Mt III forms an acute angle with the proximal facet, while the posterior facet is separated from the proximal border. The diaphysis is slightly curved medially, becoming slightly larger distally, with small differences between its maximal and articular distal widths (Supplementary Material S1: Table S26). The anterior border of the proximal facet of Mt III (Figure 6 (7)) is straight and curves laterally, while the medial and lateral borders of the diaphysis diverge slightly distally. Mt IV (Figure 6 (8)) is straighter than Mt II. The proximal epiphysis is trapezoidal, with some torsion with respect to the distal epiphysis. Medially, the anterior facet of Mt III is subtriangular while its posterior facet is rounded.

The size and gracility of Mt II are similar to those of the Mt II from Vallonet and Pietrafitta [31,61], while the metatarsal from Hunsheim is larger and more robust. Those from Untermassfeld are longer, but the gracility index lies between those of CR and Hunsheim (Supplementary Material S1: Table S26; Supplementary Material S2). The length of Mt III is similar to the minimum value for *S. hundsheimensis* provided by Guérin [29] and is clearly shorter than the Mt III from Hunsheim [34]. The gracility index values of CR lie between those from Voigtstedt (more slender) and Isernia (the most robust) (Supplementary Material S1: Table S27; Supplementary Material S2). The length of Mt IV is actually below that of the minimum length proposed [29] and the gracility index values of the right and left bones differ, with the index of the left bone being more similar to those of most of the specimens of *S. hundsheimensis* in the comparison, with the exception of those from Voigtstedt, which is the slenderest (Supplementary Material S1: Table S28; Supplementary Material S2).

#### 4.2.10. Phalanges

Various first, second, and third phalanges were recovered and measured, but we were unable to identify which digit they belonged to (Supplementary Material S1: Table S29). Some of the phalanges of individual # 8661 are anatomically connected to their metacarpals (Figure 1 (6)).

### 5. Discussion

#### 5.1. Taxonomy

The comparison reported herein—based, on this occasion, on a larger sample—supports the previous assignment of some of the rhinoceros remains from CR to *Stephanorhinus hundsheimensis*. As discussed, the general morphology of the remains, in particular that of the skull (with a long, moderate occipital height, partial nasal septum, slender zygomatic arch, and less-developed nasal horn base), allows us to discard other late Middle–Upper Pleistocene species from consideration, including *S. hemitoechus*, *S. kirchbergensis*, and *Coelodonta antiquitatis*. *Stephanorhinus etruscus*, which did not survive until the late Middle Pleistocene, presents greater general similarities, but the species differs, for instance, insofar as the lateral borders of its occipital face are more vertical and the dorsal corners more angled (for detailed comparisons with this species see [3,29,30], among others). It is often difficult to differentiate between the species of *Stephanorhinus* on the basis of their dental features, while *S. hundsheimensis* and *S. hemitoechus* overlap considerably in terms of their size. Yet, the remains from CR provide a better overall fit with *S. hundsheimensis*, being similar in this regard to materials from Hunsheim (the type locality) and Isernia.

The postcranial elements of the CR specimens present similarities with *S. hundsheimensis* remains from various sites, including those of Hunsheim, Untermassfeld, Voigtstedt, Süssenborn, and Isernia, among others. Despite their overlapping sizes, the bones of *S. hemitoechus* are generally larger (at least, as regards most of their mean values); moreover, various differences in their general morphology or articular facets are observed (see discussion above). Fortelius et al. [30] concluded that the skeleton of *S. hundsheimensis* is slightly

larger than, albeit quite similar in certain respects to, that of *S. etruscus*, but with bones that are in some cases more robust. Compared to *S. hemitoechus*, the metapodials are usually shorter in the latter, with broader distal epiphyses in the Mc III and Mt III. Our bivariate plots, however, do not reveal a clear proportional differentiation in the studied material but do point to the generally smaller size of *S. hundsheimensis*.

### 5.2. Biostratigraphy

Evidence of the presence of *Stephanorhinus hundsheimensis* at CR can be added to the few other reports of the presence of this taxon in Spain. To date, the species has been identified in the Lower Pleistocene of Vallparadís and Incarcàl in the northeast [5,13–19] and the Guadix-Baza basin in the south [20–23], in some cases ascribed originally to *S. etruscus*. During the Middle and Upper Pleistocene, the common rhinoceros documented in Spain is *S. hemitoechus* [3–5], while reports of *Coelodonta antiquitatis* are scarce [13] and the presence of *S. kirchbergensis* was largely discarded [3,12]. The presence of *S. hundsheimensis* in layers VII and IIIe of CR implies an extension of its temporal record, not only in Spain but in Europe, into the late Middle–early Upper Pleistocene, which encompasses MIS 6–7 and MIS 5. MIS 5 is particularly interesting as it includes substage MIS 5e (Eemian), which corresponds to the last Pleistocene interglacial period, and the presence of *S. hundsheimensis* during this stage would correspond to the most recent record of this species in Europe. Other European sites corresponding to, or including, this period are found in Italy: Madonna dell’Arma [62], Caverna degli Orsi [63], San Sidero 3 [64], Grotta Grande of Scario [65], and Grotta degli Orsi Volante [66]; however, the occurrence of *S. hundsheimensis* has not been recorded.

In addition to *S. hundsheimensis*, the taxonomic assemblage from CR sheds light on a period that is scarcely documented in the Iberian Peninsula. Indeed, other rare species as regards both their chronological and geographical distribution are recorded for the first time in the Upper Pleistocene at this site, including the cervid *Haploidoceros mediterraneus*, the ibex *Capra cf. ibex*, and the rodent *Glis glis* [10,27]. The presence of *Haploidoceros* and the ibex has been subsequently established at other Upper Pleistocene Spanish sites ([67,68] and references therein).

The oldest European records of *S. hundsheimensis* correspond to MIS 16–15 in Italy ([2,5,43]) and to MIS 15–13 in central and northern Europe [2,5,23,29,69,70], while the most recent correspond to sites in Georgia and Armenia [31,71–73].

Lacombat [31] provides a summary of the biochronological distribution of *S. hundsheimensis* and accompanying large mammal species. The author relates the extinction of this rhinoceros to that of *Equus suessembornensis* and *Macaca sylvana sylvana*, as well as to the appearance of *Mammuthus primigenius*, *Equus hydruntinus*, *Dama dama*, and *Capra ibex*. The smaller, older form (the first evolutionary stage) of *S. hundsheimensis* was coeval with Villafranchian and Galerian large mammal species, whereas the larger, later form (the second evolutionary stage) cohabited only with Galerian species [31].

### 5.3. Geographical Distribution

*Stephanorhinus hundsheimensis* presents a wide geographical distribution. Pandolfi et al. [37] (see [37] (Figure 1)) summarized the areas where the species has been recorded, essentially, that is, during the Lower Pleistocene. Thus, it is mainly present in Western and Eastern Europe, but also in Turkey (the Anatolian Peninsula) and the Caucasus. Early Middle Pleistocene sites have also been described in Austria, England, Germany, France, Italy, and Spain.

The distribution of *S. hundsheimensis* is more homogeneous than that of *S. hemitoechus*, which is predominant in Mediterranean areas, and *S. kirchbergensis*, which is predominant in central Europe. *S. hundsheimensis* was, likewise, more ubiquitous, being readily adaptable to different environments and feeding methods [69,74]. This species would have replaced the last isolated populations of *S. etruscus* [75]. Guérin [29] differentiated between two evolutionary stages of *S. etruscus*—one based on the Early–Middle Villafranchian materials and

the other on those of the Late Villafranchian (*S. e. brachycephalus* = *S. hundsheimensis*)—with a general variation in body size. Size variation was also detected among *S. hundsheimensis* [29,31]. Lacomat [31,69] associated the two different sizes described for this species with palaeoenvironmental conditions. On the whole, representatives of *S. hundsheimensis* from the Lower Pleistocene (late Villafranchian–early Galerian) are smaller (similar in size to *S. etruscus*) than those from the early Middle Pleistocene [31], but the size difference is also related to the species' geographical distribution [69]. Thus, when comparing sites of equivalent age, Lacomat [69] established that those specimens from southern sites, such as Vallonet (France), are clearly smaller than those from the northern Untermassfeld (Germany). Yet, this German sample presents a similar size to that of the more recent, southern site of Isernia (Italy; Middle Pleistocene). On these grounds, the author [69] identifies two geographical areas, each of which presents an increasing specimen size over time.

Consequently, the more recent remains from CR should be larger; however, they are not especially large, even if we only take into consideration the measurements of the full adult specimen. For instance, the skull measurements of individual # 8096 are mostly below the mean values established by Guérin [29]; the mandible fragment is similar in size to those of the specimens from Isernia, and the upper M3 and lower premolars reach the maximum values presented by specimens from Vallonet and Isernia. Moreover, among the postcranial bones, the Mc III, for instance, is shorter than those from Vallonet, Untermassfeld, Soleilhac, and Voigtstedt, while the gracility index values are similar; Mt III is shorter than those of all the specimens compared and the gracility index is slightly higher than those from Hundsheim and Voigtstedt, but lower than that of Isernia, and the astragalus is smaller than those from Isernia albeit more similar to those from Vallonet (see Supplementary Material S1 and comparisons above). However, the size variations within *S. hundsheimensis* can be great and not all the measurements here point to the markedly smaller size of the remains from CR. Indeed, the relatively small overall size of the CR remains might be related to the geographical location of this site in southern Europe. Indeed, a relatively small size has been established for the Spanish sample of the species *S. hemitoechus* with respect to other European populations [3], a condition that might be more attributable to its geographical isolation than to the prevailing palaeoenvironmental conditions [10].

#### 5.4. Palaeobiological Remarks

According to Fortelius et al. [30], the long limbs, brachydont dentition, and head posture of *S. hundsheimensis* (as well as *S. etruscus*) suggest that this rhinoceros browsed on vegetation of intermediate height in open habitats. *S. hundsheimensis* was, however, a larger, less cursorial animal, with a longer face and greater horns, than *S. etruscus*. During the latest Lower Pleistocene, these two species were coeval but present at different sites (with the exception of Trlica, although the remains correspond to different stratigraphic levels [52]), which might be attributable to their favouring distinct habitats [37]. Pandolfi et al. [37] described two skulls from Dmanisi, Georgia, where both *S. etruscus* and *S. hundsheimensis* had been identified, but an in-depth taxonomic study of the complete rhinocerotid sample had yet to be conducted. The morphometric study reported by these authors [37] assigned the skulls to two distinct morphotypes, unrelated to intraspecific variability or sexual dimorphism, but rather to a niche partitioning based on feeding habitats, putatively interpretable as two species or two ecomorphotypes of the same species. Mesowear analyses on teeth [74] have revealed that *S. hundsheimensis* was the most ecologically flexible of the Plio–Pleistocene rhinoceroses and a mixed-feeder, fluctuating between a browse- and a graze-dominated diet [37]. This interpretation agrees with the inferred landscape for CR, that is, a mixed wooded vegetation with temperate climatic conditions [10].

In contrast, *S. hemitoechus* had shorter limbs, hypsodont molars, and weaker horns [30]. According to Pandolfi et al. ([43] and references therein), the appearance of *S. hemitoechus* in Europe during MIS 13 coincides with an increase in abrasive herbaceous vegetation in a progressively arid period.

The three individuals recovered from CR correspond to three quite distinct ontogenetic stages: full adult, sub-adult (with two teeth still erupting), and juvenile (with complete milk dentition). In line with some authors, including Anders et al. [76], the latter might even be considered an infant. According to data for the extant black rhinoceros [77], individual # 8096 would have been older than 22, and individual # 8661 would have been around 6–7 years old. Sanz and Daura [26], after performing a taphonomic analysis of the CR site, focused primarily on layer I, conclude that the accumulation in this layer was generated by carnivore activity. However, they conclude that the accumulations in layers III to VII (where the rhino remains were found) indicate that the site served as a trap, with a markedly vertical entrance. They base this conclusion on the presence of complete, articulated skeletons (not only of rhinos but also of a juvenile elephant and a juvenile auroch) and the absence of any biological marks (e.g., carnivore bites). Furthermore, the different ontogenetic stages represented in the case of *Stephanorhinus* also support the idea that the cavity was a natural trap ([26] and references therein).

## 6. Conclusions

The *Stephanorhinus hundsheimensis* record at the Cova del Rinoceront points to the persistence of this rhinoceros up to MIS 5-6. The morphological comparison conducted herein of the CR specimens—especially their skull characteristics but also their mandibular, dental, and postcranial features—allows us to confirm this preliminary taxonomic determination of the first recovered remains. This record, however, contrasts with the common species identified in the late Middle-Early Upper Pleistocene of southwestern Europe, namely, that of *S. hemitoechus*.

It is not possible to determine with any degree of precision the date of the disappearance of *S. hundsheimensis* from the northeastern Iberian Peninsula. No rhino remains are present in the uppermost layers of CR (I to III<sub>d</sub>), dated between MIS 5a and MIS 5d, while more recent remains in the area surrounding the Garraf Massif correspond to *S. hemitoechus* and *Coelodonta antiquitatis*, associated with MIS 4-3 and the Heinrich Stadial 4. As such, the disappearance of *S. hundsheimensis* may have occurred between the boundary of MIS 5 and MIS 4.

The recognition of *S. hundsheimensis* at the Cova del Rinoceront cannot be understood as an isolated occurrence, at least, as far as the Iberian Peninsula is concerned. The three individuals recovered from CR support claims that this species may well have been more widespread than previously believed. Moreover, the younger-than-expected record of *S. hundsheimensis* at CR raises a new question about current biostratigraphic/geographical distribution. As our comparative study highlights, the morphological variations and the overlapping of sizes make it difficult, on occasion, to separate *S. hundsheimensis* from *S. hemitoechus* with any degree of confidence, especially when based on partial remains. This means that the misidentification of other rhino samples cannot be altogether ruled out and that an in-depth revision is perhaps required to provide a better understanding of the presence of *S. hundsheimensis* in the Late Pleistocene. Moreover, various factors, including a climatic influences and the refugia conditions of the Iberian Peninsula might also be related to the rhino's occurrence.

**Supplementary Materials:** The following supporting information can be downloaded at <https://www.mdpi.com/article/10.3390/quat6040060/s1>, Supplementary Material S1: Tables S1–S29: Dimensions (in millimetres) of the skull, mandible, dentition, and postcranial bones of *S. hundsheimensis* from Cova del Rinoceront compared with those of other *Stephanorhinus* remains. Supplementary Material S2: Bivariate plots showing comparative proportions of certain bones (humerus, femur, radius, tibia, Mc II, Mc III, astragalus, calcaneus, Mt II, and Mt IV) of *S. hundsheimensis* from Cova del Rinoceront based on data provided in the corresponding tables. Abbreviations of sites in the plots correspond to complete names in the tables. S.h., *Stephanorhinus hundsheimensis*; S.he., *S. hemitoechus*; S.e., *S. etruscus*. References [78,79] are cited in the supplementary materials.

**Author Contributions:** All authors designed research and wrote the paper. D.G.-F. first described the paleontological remains. E.C. reviewed, edited, and analysed the paleontological data. M.S. and J.D. conducted the archaeological work, the curation of the material, organized the collection for the paleontological study, provided contextual information and the figures illustrating the rhino material and the site. All authors have read and agreed to the published version of the manuscript.

**Funding:** This research benefited from financial support from the following agencies: a *Ramon y Cajal* postdoctoral grant (RYC2021-032999-I, M.S.) funded by the *Ministerio de Ciencia e Innovación* and the European Union-NextGenerationEU; the *Departament de Cultura de la Generalitat de Catalunya* (grant no. CLT/2022/ARQ001SOLC/128) and AGAUR (SGR2021-00337); the *Ministerio de Ciencia e Innovación*, government of Spain (PID2020-113960GB-I00/AEI/10.13039/501100011033); and the CNRS-INEE International Research Network program (grant no. IRN0871TaphEN). Fieldwork and fossil preparation were sponsored by the *Ajuntament de Castelldefels*.

**Data Availability Statement:** All data generated during this study are included in this published article and its supplementary information files.

**Acknowledgments:** Special thanks are due to L. Pandolfi for the invitation (to EC) to participate in this volume on Quaternary mammals; to C.I. Montalvo (Universidad Nacional de La Pampa, Argentina), for her comments on bioerosion marks; and to M. Roig for helping with the bivariate plots. Thanks to Claude Guérin for the initial identification of the specimen #8096 as *Dicerorhinus etruscus brachycephalus* when the site was discovered in 2003. Almudena S. Yagüe and Blanca Sicilia were responsible for the cleaning and restoring of the specimens.

**Conflicts of Interest:** The authors declare no conflict of interest.

## References

- Pandolfi, L. *Sistematica e Filogenesi dei Rhinocerotini (Mammalia, Rhinocerotidae)*. Ph.D. Dissertation, Scuola Dottorale in Geologia dell'Ambiente e delle Risorse, Università degli Studi Roma Tre, Roma, Italy, 2015; p. 338.
- Pandolfi, L.; Erten, H. *Stephanorhinus hundsheimensis* (Mammalia, Rhinocerotidae) from the late early Pleistocene deposits of the Denizli Basin (Anatolia, Turkey). *Geobios* **2017**, *50*, 65–73. [[CrossRef](#)]
- Cerdeño, E. *Stephanorhinus hemitoechus* (Falc.) (Rhinocerotidae, Mammalia) del Pleistoceno medio y superior de España. *Est. Geol.* **1990**, *46*, 465–479. [[CrossRef](#)]
- Riquelme Cantal, J.A.; Barroso Ruiz, C.; Botella Ortega, D.; Caparrós, M.; Moine, A.M.; García Solano, J.A. Un yacimiento del Pleistoceno medio y superior en el sur de la Península Ibérica: La Cueva del Ángel (Lucena, Córdoba). *CPAG* **2010**, *20*, 201–221.
- Pandolfi, L.; Marra, F. Rhinocerotidae (Mammalia, Perissodactyla) from the chrono-stratigraphically constrained Pleistocene deposits of the urban area of Rome (Central Italy). *Geobios* **2015**, *699*, 147–167. [[CrossRef](#)]
- Zilhão, J.; Angelucci, D.E.; Arnold, L.J.; Demuro, M.; Hoffmann, D.L.; Pike, A.W.G. A revised, Last Interglacial chronology for the Middle Palaeolithic sequence of Gruta da Oliveira (Almonda karst system, Torres Novas, Portugal). *Quat. Sci. Rev.* **2021**, *258*, 106885. [[CrossRef](#)]
- Zilhão, J.; Angelucci, D.E.; Araújo Igreja, M.; Arnold, L.J.; Badal, E.; Callapez, P.; Cardoso, J.L.; d'Errico, F.; Daura, J.; Demuro, M.; et al. Last Interglacial Iberian Neandertals as fisher-hunter-gatherers. *Science* **2020**, *367*, eaaz7943. [[CrossRef](#)] [[PubMed](#)]
- Demuro, M.; Arnold, L.J.; Aranburu, A.; Gómez-Olivencia, A.; Arsuaga, J.L. Single-grain OSL dating of the Middle Palaeolithic site of Galería de las Estatuas, Atapuerca (Burgos, Spain). *Quat. Geochr.* **2019**, *49*, 254–261. [[CrossRef](#)]
- Arsuaga, J.L.; Baquedano, E.; Pérez-González, A.; Sala, M.T.; Quam, R.M.; Rodríguez, L.; García, R.; García, N.; Álvarez-Lao, D.; Laplana, C.; et al. Understanding the ancient habitats of the last-interglacial (late MIS 5) Neanderthals of central Iberia: Paleoenvironmental and taphonomic evidence from the Cueva del Camino (Spain) site. *Quat. Intern.* **2012**, *275*, 55–75. [[CrossRef](#)]
- Daura, J.; Sanz, M.; Julià, R.; García-Fernández, D.; Fornós, J.J.; Vaquero, M.; Allué, M.; López-García, J.M.; Blain, H.A.; Ortiz, J.E.; et al. Cova del Rinoceront (Castelldefels, Barcelona): A terrestrial record for the Last Interglacial period (MIS 5) in the Mediterranean coast of the Iberian Peninsula. *Quat. Sci. Rev.* **2015**, *114*, 203–227. [[CrossRef](#)]
- Pandolfi, L.; Tagliacozzo, A. *Stephanorhinus hemitoechus* (Mammalia, Rhinocerotidae) from the Late Pleistocene of Valle Radice (Sora, Central Italy) and re-evaluation of the morphometric variability of the species in Europe. *Geobios* **2015**, *48*, 169–191. [[CrossRef](#)]
- Van der Made, J. The rhinos from the Middle Pleistocene of Neumark-Nord (Saxony-Anhalt). *Veröffentlich. Land. Denkm. Archäol.* **2010**, *62*, 433–527.
- Álvarez-Lao, D.J.; García, N. Southern dispersal and Palaeoecological implications of woolly rhinoceros (*Coelodonta antiquitatis*): Review of the Iberian occurrences. *Quat. Sci. Rev.* **2011**, *30*, 2002–2017. [[CrossRef](#)]
- Alba, D.M.; Aurell, J.; Madurell, J.; Gómez, M.; Moyà-Solà, S.; Berástegui, X. Paleontologia i Geologia del jaciment del Pleistocè inferior de Vallparadís (Terrassa, Vallès Occidental). *Trib. d'Arqueol.* **2008**, *2008*, 29–44.

15. Madurell-Malapeira, J.; Minwer-Barakat, R.; Alba, D.M.; Garcés, M.; Gómez, M.; Aurell-Garrido, J.; Ros-Montoya, S.; Moyà-Solà, S.; Berástegui, X. The Vallparadis section (Terrassa, Iberian Peninsula) and the latest Villafranchian faunas of Europe. *Quat. Sci. Rev.* **2010**, *29*, 3972–3982. [[CrossRef](#)]
16. Madurell-Malapeira, J.; Ros-Montoya, M.P.; Espigares, D.M.; Alba, J.; Aurell-Garrido, J. Villafranchian large mammals from the Iberian Peninsula: Paleobiography, paleoecology and dispersal events. *J. Iber. Geol.* **2014**, *40*, 167–178. [[CrossRef](#)]
17. Alba, D.M.; Madurell-Malapeira, J.; Nelson, E.; Vinuesa, V.; Susana, I.; Patrocínio Espigares, M.; Ros-Montoya, S.; Martínez-Navarro, B. First record of macaques from the Early Pleistocene of Incarcal (NE, Iberian Peninsula). *J. Hum. Evol.* **2016**, *96*, 139–144. [[CrossRef](#)]
18. García-Fernández, D.; Galobart, A.; Ros, X.; Cerdeño, E. *Stephanorhinus etruscus* (Rhinocerotidae) en el Villafranchiense de Crespia (Girona, NE de la Península Ibérica). *Paleontol. Evol.* **2001**, *34*, 279–296.
19. García-Fernández, D.; Galobart, A.; Cerdeño, E. Perisodáctilos del Pleistoceno inferior de los yacimientos de Incarcal (Girona, NE de la Península Ibérica). *Paleontol. Evol.* **2003**, *34*, 175–183.
20. Cerdeño, E. Remarks on the Spanish Plio-Pleistocene rhinocerotid *Stephanorhinus etruscus*. *Comptes Rendus Acad. Sci. Paris* **1993**, *317*, 1363–1367.
21. Ros Montoya, S. Los Proboscídeos del Plio-Pleistoceno de las Cuencas de Guádix-Baza y Granada. Doctoral Thesis, Departamento de Estratigrafía y Paleontología, Universidad de Granada, Granada, Spain, 2010.
22. Lacombat, F. Estudio paleontológico de *Stephanorhinus hundsheimensis* de Fuente Nueva 3 y Barranco León. In *Ocupaciones Humanas en el Pleistoceno Inferior y Medio de la Cuenca Guadix-Baza*; Toro, I., Martínez-Navarro, B., Agustí, J., Eds.; Junta de Andalucía, Arqueología-Monografías: Sevilla, Spain, 2010; pp. 237–246.
23. Duval, M.; Falgueres, C.; Bahain, J.J.; Rainer Gru, N.; Qinfeng, S.; Maxime, A.; Hellstrom, J.; Dolo, J.M.; Agustí, J.; Martínez-Navarro, B.; et al. The challenge of dating Early Pleistocene fossil teeth by the combined uranium series–electron spin resonance method: The Venta Micena palaeontological site (Orce, Spain). *J. Quat. Sci.* **2011**, *26*, 603–615. [[CrossRef](#)]
24. Rodríguez-Gómez, G.; Rodríguez, J.; Mateos, A.; Martín-González, J.A.; Goikoetxea, I. Food Web Structure during the European Pleistocene. *J. Taphon.* **2012**, *10*, 165–184.
25. Daura, J.; Sanz, M. El jaciment prehistòric de la pedrera de Ca n’Aymerich de Castelldefels. IV Trobades d’Estudiosos del Massís del Garraf (21 de novembre de 2002, Vilanova i al Geltrú). *Diput. Barc. Serv. Parcs Nat. Monogr.* **2004**, *37*, 165–168.
26. Sanz, M.; Daura, J. Taphonomic analysis of an ungulate-dominated accumulation at the Pleistocene Cova del Rinoceront site near Barcelona, Spain (northeastern Iberian Peninsula). *Palaeogeogr. Palaeoclimatol. Palaeoecol.* **2018**, *498*, 24–38. [[CrossRef](#)]
27. Croitor, R.; Sanz, M.; Daura, J. The endemic deer *Haploidoceros mediterraneus* (Bonifay) (Cervidae, Mammalia) from the Late Pleistocene of Cova del Rinoceront (Iberian Peninsula): Origin, ecomorphology, and paleobiology. *Hist. Biol.* **2020**, *32*, 409–427. [[CrossRef](#)]
28. Palombo, M.R.; Sanz, M.; Daura, J. The complete skeleton of a straight-tusked elephant calf from Cova del Rinoceront (Late Pleistocene, NE Iberian Peninsula): New insights into ontogenetic growth in *Palaeoloxodon antiquus*. *Quat. Sci. Rev.* **2021**, *274*, 107257. [[CrossRef](#)]
29. Guérin, C. Les Rhinocerotidae (Mammalia-Perissodactyla) du Miocene Terminal au Pléistocène supérieur d’Europe Occidentale comparación avec les especes actuelles. *Doc. Lab. Géol. Lyon* **1980**, *79*, 1–1185.
30. Fortelius, M.; Mazza, P.; Sala, B. *Stephanorhinus* (Mammalia-Rhinocerotidae) of the Western European Pleistocene, with a revision of *S. etruscus* (Falconer, 1868). *Palaeontogr. Ital.* **1993**, *80*, 63–155.
31. Lacombat, F. *Les Rhinocéros Fossiles des Sites Préhistoriques de l’Europe Méditerranéenne et du Massif Central, Paléontologie et Implications Bichronologiques*; British Archaeological Reports, International Series, 1419; BAA: Oxford, UK, 2005; pp. 1–175.
32. Geraads, D.; Cerdeño, E.; García Fernández, D.; Pandolfi, L.; Billia, E.; Athanassiou, A.; Albayrak, E.; Codrea, V.; Obada, T.; Deng, T.; et al. A Database of Old-World Neogene and Quaternary Rhino-Bearing Localities. 2020. Available online: <http://www.rhinosourcecenter.com/about/fossil-rhino-database.php> (accessed on 15 February 2023).
33. von Jäger, G.F. *Über die Fossilen Säugethiere, Welche in Württemberg in Verschiedenen Formationen Aufgefunden Worden Sind, Nebst Geognostischen Bemerkungen über Diese Formationen*; Carl Erhard: Stuttgart, Germany, 1839; p. 214.
34. Toulou, F. Das Nashorn von Hundsheim *Rhinoceros (Ceratorhinus Osborn) Hundsheimensis* nov. form. Mit Ausführungen über die Verhältnisse von elf Schädeln von *Rhinoceros (Ceratorhinus) sumatrensis*. *Abh. KK Geol. Reich.* **1902**, *19*, 1–92.
35. Mazza, P. The Tuscan Early Pleistocene *Dicerorhinus etruscus*. *Palaeontogr. Ital.* **1988**, *75*, 1–87.
36. Azzaroli, A. Validità della specie *Rhinoceros hemitoechus* Falc. *Palaeont. Ital.* **1962**, *57*, 21–34.
37. Pandolfi, L.; Bartolini-Lucenti, S.; Cirilli, O.; Bukhsianidze, M.; Lordkipanidze, D.; Rook, L. Paleoecology, biochronology, and paleobiogeography of Eurasian Rhinocerotidae during the Early Pleistocene: The contribution of the fossil material from Dmanisi (Georgia, Southern Caucasus). *J. Hum. Evol.* **2021**, *156*, 103013. [[CrossRef](#)] [[PubMed](#)]
38. Kotowski, A.; Stefaniak, K.; Kahlke, R.-D. A rhinocerotid skull from the Early Pleistocene site of Untermassfeld. In *The Pleistocene of Untermassfeld near Meiningen (Thüringen, Germany)*; Kahlke, R.-D., Ed.; Römisch-Germanisches Zentralmuseum: Mainz, Germany, 2020; Part 4; pp. 273–1294.
39. Loose, H.K. Pleistocene Rhinocerotidae of W. Europe with reference to the recent two-horned species of Africa and S.E. Asia. *Scr. Geol.* **1975**, *33*, 1–60.
40. Schreiber, H.D. Osteological investigations on skeleton material of Rhinoceroses (Rhinocerotidae, Mammalia) from the Early Middle Pleistocene locality of Mauer near Heidelberg (SW-Germany). *Quat. Hors Série* **2005**, *2*, 103–111.

41. Cigala-Fulgosi, F. *Dicerorhinus hemitoechus* (Falconer) del post-villafranchiano fluviolacustre del Torrente Stirone (Salsomaggiore, Parma). *Boll. Soc. Paleontol. Ital.* **1976**, *15*, 59–72.
42. Bona, F.; Sala, B. Villafranchian-Galerian mammal faunas transition in South-Western Europe. The case of the Late Early Pleistocene mammal fauna of the Frantoio locality, Arda River (Castell'Arquato, Piacenza, Northern Italy). *Geobios* **2016**, *49*, 329–347. [[CrossRef](#)]
43. Pandolfi, L.; Gaeta, M.; Petronio, C. The skull of *Stephanorhinus hemitoechus* (Mammalia, Rhinocerotidae) from the Middle Pleistocene of Campagna Romana (Rome, central Italy): Biochronological and paleobiogeographic implications. *Bull. Geosci.* **2013**, *88*, 51–62. [[CrossRef](#)]
44. Schroeder, H. Die Wirbelthier-Fauna des Mosbacher Sandes. 1. Gattung *Rhinoceros*. *Abh. Kön. Preuss. Geol. Landes.* **1903**, *18*, 1–143.
45. Kahlke, H.D. Die Rhinocerotiden-Reste aus den Tonen von Voigtstedt in Thüringen. *Palaeontol. Abh. A* **1965**, *2*, 451–520.
46. Sala, B.; Fortelius, M. The Rhinoceros of Isernia La Pineta (early Middle Pleistocene, Southern Italy). *Palaeontogr. Ital.* **1993**, *80*, 157–174.
47. Mazza, P. The Middle Pleistocene rhinoceros remains from Cesi (Colfiorito Basin, Macerata, Central Italy). *Boll. Soc. Paleontol. Ital.* **1996**, *35*, 349–355.
48. Kahlke, H.D. Die Rhinocerotiden-Reste aus den Kiesen von Süssenborn bei Weimar. *Palaeontol. Abh. A* **1969**, *3*, 667–709.
49. Kahlke, H.D. Die Rhinocerotiden-Reste aus dem unterpleistozän von Untermassfeld. In *Das Pleistozän von Untermassfeld bei Meiningen, Thüringen*; Kahlke, R.-D., Ed.; Monographien Römisch-Germanischen Zentralmus: Mainz, Germany, 2001; Volume 40, pp. 501–556.
50. Moullé, P.E.; Lacombat, F.; Echassoux, A. Apport des grands mammifères de la Grotte du Vallonet (Roquebrune-Cap Martin, Alpes Maritimes, France) à la connaissance du cadre biochronologique de la seconde moitié du Pléistocène inférieur d'Europe. *L'Anthropologie* **2006**, *110*, 837–849. [[CrossRef](#)]
51. Ballatore, M.; Breda, M. *Stephanorhinus hundsheimensis* (Rhinocerotidae, Mammalia) teeth from the early Middle Pleistocene of Isernia La Pineta (Molise, Italy) and comparison with coeval British material. *Quat. Intern.* **2013**, *302*, 169–183. [[CrossRef](#)]
52. Vislobokova, I.A.; Agadjanian, A.K. New data on large mammals of the Pleistocene Trlica Fauna, Montenegro, the Central Balkans. *Paleontol. J.* **2015**, *49*, 651–667. [[CrossRef](#)]
53. Cerdeño, E. Presencia de rinoceronte en la fauna de Cueva Millán (Burgos). *Geogaceta* **1987**, *2*, 9–10.
54. Lacombat, F. Morphological and biometrical differentiation of the teeth from the Pleistocene species of *Stephanorhinus* (Mammalia, Perissodactyla, Rhinocerotidae) in Mediterranean Europe and the Massif Central, France. *Palaeontographica A* **2006**, *274*, 71–111. [[CrossRef](#)]
55. Alférez, F.; Íñigo, C. Los restos de *Dicerorhinus hemitoechus* (Perissodactyla; Mammalia) del Pleistoceno Medio de Pinilla del Valle (Madrid). In *Actas de Paleontología*; Civis Llovera, J., Flores Villarejo, A., Eds.; Universidad de Salamanca: Salamanca, Spain, 1990; pp. 25–40.
56. Íñigo, C. El rinoceronte del Pleistoceno Superior de la Cueva del Búho (Segovia). *Bol. Geol. Min.* **1995**, *106*, 107–110.
57. Van der Made, J.; Montoya, P. Rinocerontes del Pleistoceno de El Bardello, Plaça de La República y El Molinar en Alcoy, España. *Rev. Mus. Alcoi* **2007**, *16*, 7–18.
58. Abdala, V.; Vera, M.C.; Amador, L.I.; Fontanarrosa, G.; Fratani, J.; Ponssa, M.L. Sesamoids in tetrapods: The origin of new skeletal morphologies. *Biol. Rev.* **2019**, *94*, 2011–2032. [[CrossRef](#)]
59. Baryshnikov, G.; Guérin, C.; Mezhlumyan, S.K. Rhinoceros *Dicerorhinus etruscus brachycephalus* from the Yerevan Mousterian site. *Proc. Zool. Inst.* **1989**, *198*, 103–110.
60. Santafé, J.V.; Casanovas, M.L. *Dicerorhinus hemitoechus* (Falconer, 1868) (Mammalia, Perissodactyla) del yacimiento Pleistocénico de la Cova del Gegant (Garraf, Barcelona). *Empúries* **1986**, *48–50*, 310–322.
61. Mazza, P.; Sala, B.; Fortelius, M. A small latest Villafranchian (late Early Pleistocene) rhinoceros from Pietrafitta (Perugia, Umbria, Central Italy) with notes on the Pirro and Westerhoven rhinoceroses. *Palaeontogr. Ital.* **1993**, *8*, 25–50.
62. Kaniewski, D.; Renault-Miskovskiy, J.; de Lumley, H. Palaeovegetation from a *Homo neanderthalensis* occupation in Western Liguria: Archaeopalynology of Madonna dell'Arma (San Remo, Italy). *J. Archaeol. Sci.* **2005**, *32*, 827–840. [[CrossRef](#)]
63. Berto, C.; Rubinato, G. The upper Pleistocene mammal record from Caverna degli Orsi (San Dorligo della Valle–Dolina, Trieste, Italy): A faunal complex between eastern and western Europe. *Quat. Int.* **2013**, *284*, 7–14. [[CrossRef](#)]
64. Petronio, C.; Pandolfi, L. *Stephanorhinus hemitoechus* (Falconer, 1868) del Pleistocene superiore dell'area di Melpignano-Cursi e S. Sidero (Lecce, Italia). *Geol. Romana* **2008**, *41*, 1–12.
65. Ronchitelli, A.; Abbazzzi, L.; Accorsi, A.A.; Bandini Mazzanti, M.; Bernardi, M.; Masini, F.; Mercuri, A.; Mezzabotta, C.; Rook, L. The Grotta Grande of Scario (Salerno-southern Italy): Stratigraphy, archaeological finds, pollen and mammals. In Proceedings of the 1st International Congress on 'Science and Technology for the Safeguard of Cultural Heritage in the Mediterranean Basin', Siracusa, Italy, 27 November–2 December 1995.
66. Mazza, B.; Rustioni, M.; Agostini, S.; Rossi, A. An unexpected Late Pleistocene macaque remain from Grotta degli Orsi Volanti (Rapino, Chieti, Central Italy). *Geobios* **2005**, *3*, 211–217. [[CrossRef](#)]
67. van der Made, J.; Mazo, A.V. *Los Grandes Mamíferos del yacimiento de PRERESA*; Museo Arqueológico Regional, Alcalá de Henares: Comunidad de Madrid, Spain, 2014; pp. 40–67.
68. Crégut-Bonnoure, E.; Fernandez, P. Perspectives morphométriques et phylogéniques du genre *Capra* au Pléistocène (Mammalia, Artiodactyla, Caprinae). *Quaternaire* **2018**, *29*, 243–254. [[CrossRef](#)]

69. Lacombat, F. Biochronologie et grands mammifères au Pléistocène moyen et supérieur en Europe Occidentale: L'apport des Rhinocerotidae (Genre *Stephanorhinus*). *Quaternaire* **2009**, *20*, 429–435. [[CrossRef](#)]
70. Breda, M.; Collinge, S.E.; Parfitt, S.A.; Lister, A.M. Metric analysis of ungulate mammals in the early Middle Pleistocene of Britain, in relation to taxonomy and biostratigraphy. I. Rhinocerotidae and Bovidae. *Quat. Intern.* **2010**, *228*, 136–156. [[CrossRef](#)]
71. Guérin, C.; Baryshnikov, G.F. Le rhinocéros acheuléen de la grotte de Koudaro I (Géorgie, URSS) et le problème des espèces relictées du Pléistocène du Caucase. *Geobios* **1987**, *20*, 389–396. [[CrossRef](#)]
72. Baryshnikov, G.F. Local biochronology of Middle and Late Pleistocene mammals from the Caucasus. *J. Theriol.* **2002**, *1*, 61–67. [[CrossRef](#)]
73. Hoffecker, J.F.; Baryshnikov, G.F.; Doronichev, V.B. Large mammal taphonomy of the Middle Pleistocene hominid occupation at Treugol'naya Cave (Northern Caucasus). *Quat. Sci. Rev.* **2003**, *22*, 595–607. [[CrossRef](#)]
74. Kahlke, H.D.; Kaiser, T. Generalism as a subsistence strategy; advantages and limitations of the highly flexible feeding traits of Pleistocene *Stephanorhinus hudsheimensis* (Rhinocerotidae, Mammalia). *Quat. Sci. Rev.* **2011**, *30*, 2250–2261. [[CrossRef](#)]
75. Pandolfi, L.; Petronio, C. *Stephanorhinus etruscus* (Falconer, 1868) from Pirro Nord (Apricena, Foggia, Southern Italy) with notes on the older late Early Pleistocene rhinoceros remains of Italy. *Riv. Ital. Paleontol. Stratigr.* **2011**, *117*, 173–187.
76. Anders, U.; von Koenigswald, W.; Ruf, I.; Smith, B.H. Generalized individual dental age stages for fossil and extant placental mammals. *Paläontol. Z.* **2011**, *85*, 321–339. [[CrossRef](#)]
77. Hitchins, P.M. Age determination of the black rhinoceros (*Diceros bicornis* LINN.) in Zululand. *S. Afr. J. Wildl. Res.* **1978**, *8*, 71–80.
78. Petronio, C. Una mandibola di rinoceronte di Ponte Galeria. *Atti Soc. Sci. Nat.* **1988**, *129*, 173–178.
79. Bonifay, M.F. *Dicerorhinus etruscus* Falc. du Pléistocène moyen des grottes de Lunel-Viel (Hérault). *Ann. Paléont.* **1973**, *59*, 79–111.

**Disclaimer/Publisher's Note:** The statements, opinions and data contained in all publications are solely those of the individual author(s) and contributor(s) and not of MDPI and/or the editor(s). MDPI and/or the editor(s) disclaim responsibility for any injury to people or property resulting from any ideas, methods, instructions or products referred to in the content.